Pure Appl. Chem., Vol. 77, No. 2, pp. 415–428, 2005.
DOI: 10.1351/pac200577020415

Complex (dusty) plasmas: Examples for applications and observation of magnetron-induced phenomena*

H. Kersten[1,‡], G. Thieme[2], M. Fröhlich[2], D. Bojic[2], D. H. Tung[2], M. Quaas[3], H. Wulff[3], and R. Hippler[2]

[1]Institute for Nonthermal Plasmaphysics (INP), F.-L.-Jahn-Strasse 19, D-17489 Greifswald, Germany; [2]Institute for Physics, University of Greifswald, Domstrasse 10a, D-17487 Greifswald, Germany; [3]Institute of Chemistry and Biochemistry, University of Greifswald, Soldmannstrasse 16/17, D-17487 Greifswald, Germany

Abstract: Low-pressure plasmas offer a unique possibility of confinement, control, and fine tailoring of particle properties. Hence, dusty plasmas have grown into a vast field, and new applications of plasma-processed dust particles are emerging.

During the deposition of thin amorphous films onto melamine formaldehyde (MF) microparticles in a C_2H_2 plasma, the generation of nanosized carbon particles was also studied. The size distribution of those particles is quite uniform.

In another experiment, the stability of luminophore grains could be improved by coating with protective Al_2O_3 films that are deposited by a plasma-enhanced chemical vapor deposition (PECVD) process using a metal-organic precursor gas. Coating of SiO_2 microparticles with thin metal layers by magnetron sputtering is also described. Especially the interaction of the microsized grains confined in a radio frequency (rf) plasma with the dc magnetron discharge during deposition was investigated. The observations emphasize that the interaction between magnetron plasma and injected microdisperse powder particles can also be used as a diagnostic tool for the characterization of magnetron sputter sources.

Keywords: dusty plasma; plasma–particle interaction; magnetron sputtering; plasma diagnostics; luminescent particles; thin film deposition.

INTRODUCTION

The interest in the field of plasma–particle interaction with regard to dusty plasmas has grown enormously during the last decade. At present, the interest is mainly caused by applied research related to materials science [1–3] and, recently, also with regard to plasma diagnostics [4–6]. But powder formation has also been a critical concern for the microelectronics industry, because dust contamination can severely reduce the yield and performance of fabricated devices. Submicron particles deposited on the surface of process wafers can obscure device regions, cause voids and dislocations, and reduce the adhesion of thin films [7,8].

*Paper based on a presentation at the 16th International Symposium on Plasma Chemistry (ISPC-16), Taormina, Italy, 22–27 June 2003. Other presentations are published in this issue, pp. 345–495.

‡Corresponding author: E-mail: kersten@inp-greifswald.de

Nowadays, dust particles are not considered as unwanted pollutants any more. Positive aspects of dusty plasmas emerged, and they even turned into production goods. Powders produced using plasma technology have interesting and potentially useful properties, e.g., very small sizes (nanometer to micrometer range), uniform size distribution, and chemical activity. Size, structure, and composition can be tailored to the specific requirements dependent on the desired application [3,6,9]. There are several links between dusty plasma physics and materials science. The trend is similar to the well-established plasma surface modification technology, except that now the surface of dust particles is the subject of treatment. Here, deposition, etching, surface activation, modification, or separation of clustered grains in the plasma are considered. In these types of processing, particles are either grown in the plasma or are externally injected for subsequent treatment (Fig. 1).

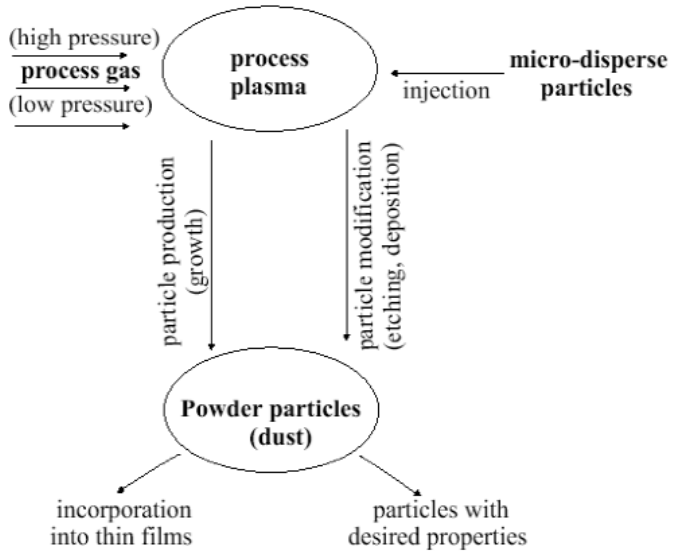

Fig. 1 Various ways of particle treatment in process plasmas.

In particular, the increased knowledge and ability to control particles in a plasma environment has recently led to new lines of technological research, namely, the tailoring of particles with desired specific surface properties.

There are numerous present and potential applications of plasma-treated particles, such as:

- treatment of soot and aerosols for environmental protection [10];
- particle synthesis in high-pressure [11–13] and low-pressure plasmas [14];
- enhancement of adhesive, mechanical, and protective properties of powder particles for sintering processes in metallurgy [15,16];
- fragmentation of powder mixtures for sorting them;
- improvement of thin film properties by incorporation of nanocrystallites for amorphous solar cells [17] and hard coatings [18,19];
- coating of lubricant particles [20];
- functionalization of microparticles for pharmaceutical and medical application;
- production of color pigments for paints;
- surface protection of phosphor particles for fluorescent lamps or electroluminescent panels [21,22];
- tailoring of optical surface properties of toner particles [9]; and
- application of processed powder particles for chemical catalysis, etc.

The interaction between plasma and injected microdisperse powder particles can also be used as a diagnostic tool for the characterization of:

- electric fields in the plasma sheath (particles as electrostatic microprobes) [23];
- energy fluxes in the plasma and toward surfaces (particles as microcalorimeters) [5,24]; and
- plasma-wall interaction (particles as microsubstrates) [25].

The idea to employ powder particles as a kind of microprobe was triggered, for example, by the basic research on the particles of plasma crystals [26,27]. Information can be obtained on the electric field and the electric potential distribution in front of electrodes and substrate surfaces by observing position and movement of the particles dependent on the discharge parameters where other plasma diagnostic methods fail.

In the present paper, some examples related to particle processing in low-pressure, low-temperature plasmas are presented, and the potential for "nonconventional" plasma diagnostics is discussed.

PARTICLE SYNTHESIS AND COATING IN AN ACETYLENE PLASMA

The production of large amounts of powders in high-pressure thermal plasma jets is at present state of the art in metal and ceramic industry [11–13]. However, size distribution and uniformity of such produced particles is mostly very poor. A solution is the use of low-pressure plasmas for powder generation and modification. But, unfortunately, particle formation in low-pressure discharges is less efficient due to the low density of active species as a result of the quite limited trapping capacity. In addition, external handling like the introduction of particles into the vacuum system and collection of processed particles raise a lot of problems. The major advantage of low-pressure plasmas is their nonequilibrium chemistry, which creates the unique possibility for fine surface treatment without damage and thermal overload. Hence, small amounts of particles with a high added value can be fabricated using low-pressure technologies. Synthesis of particles with very sharp size distributions was demonstrated by Tachibana et al. [28] who injected small carbon soot precursors into a methane plasma in order to obtain perfectly spherical objects. Vivet et al. [29] investigated an integral process of particle growth and coating in order to obtain grains with catalytic properties. In their experiments, small silicon carbide particles were produced in a SiH_4/CH_4 plasma. In the next step, the grains were coated in situ using evaporated palladium wires. Such plasma-produced particles turned out to be excellent carriers for catalytic coatings with large and active surfaces.

In our study, the synthesis of small carbon particles as well as the deposition of thin amorphous carbon (a-C:H) films onto melamine formaldehyde (MF) grains (~10 μm) in an acetylene process plasma is performed. After a very short process duration, the laser scattering remarkably increases owing to the simultaneous formation of dust in the course of a-C:H deposition.

The experiments were carried out in a reactor PULVA1, which is schematically drawn in Fig. 2. The plasma glow is located in the region between the planar aluminum radio frequency (rf) electrode (D = 130 mm) and the upper part of the spherically shaped reactor vessel (D = 400 mm) which serves as grounded electrode. The 13.56 MHz rf power is supplied by a generator (Dressler CESAR1310) in combination with an automatic matching network (Dressler VM700). The rf discharge power was varied between 5–20 W. The turbopump Pfeiffer TMU260C, which allows for a base pressure of 10^{-4} Pa, was connected to the vessel by a butterfly valve, the gas pressure was about 5 Pa. Argon and acetylene were used as process gases, the composition $Ar:C_2H_2$ was varied between 1–5. Analytical charge-coupled device (CCD) photometry (SBIG ST-6) and video recording (TELI CF8320BC) were employed to obtain information on the powder particles distributed in the plasma and illuminated by a laser fan at 532 nm (Spectra Physics MilleniaV).

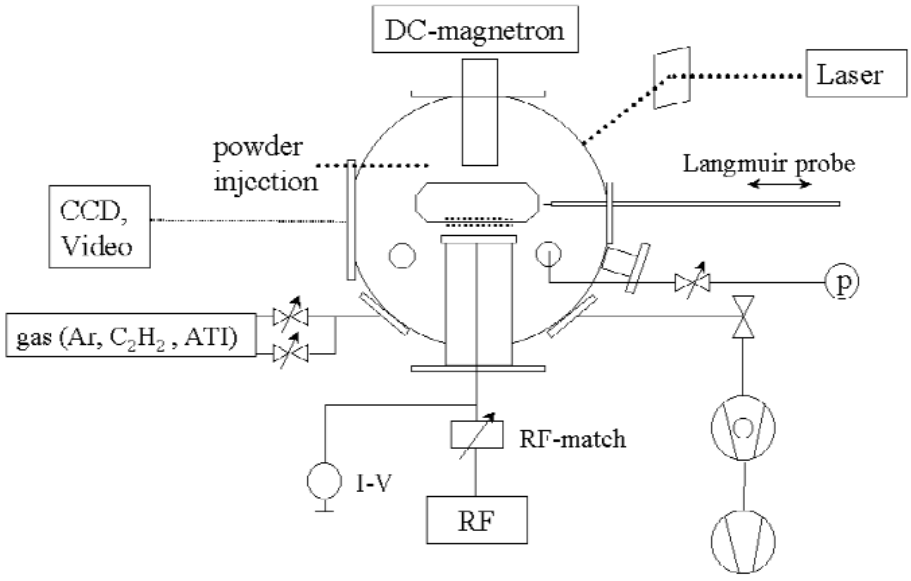

Fig. 2 Schematic of the experimental set-up PULVA1. The ion beam source on top of the reactor could be replaced by a magnetron sputter source.

Under relevant experimental conditions, there occurs not only a-C:H deposition onto the externally injected MF particles, but also the generation of small carbon dust particles. After the examination of the collected particles by scanning electron microscopy (SEM), a rather small amount of large, coated MF grains (see Fig. 3) and a huge amount of small carbon dust particles (~100 nm) can be observed. Unexpectedly, the carbon dust particles show almost the same size and form clusters, see Fig. 4.

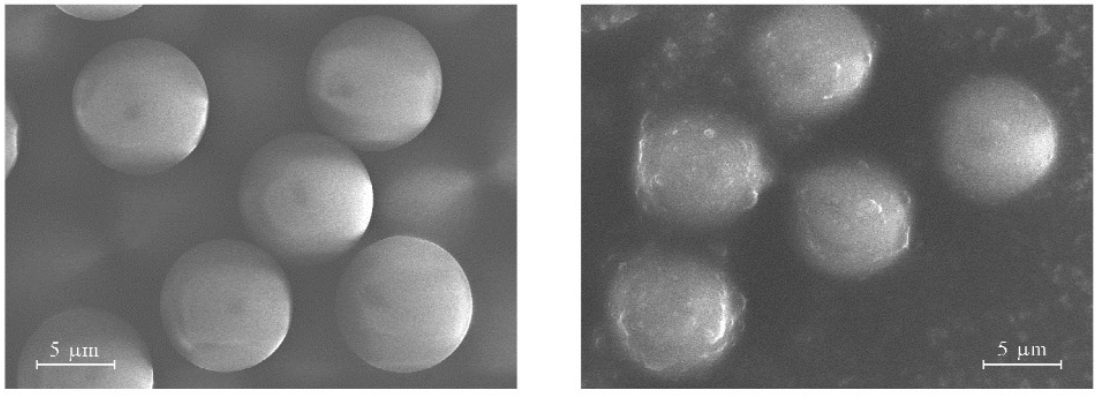

Fig. 3 MF microparticles: original (left) and a-C:H coated (right).

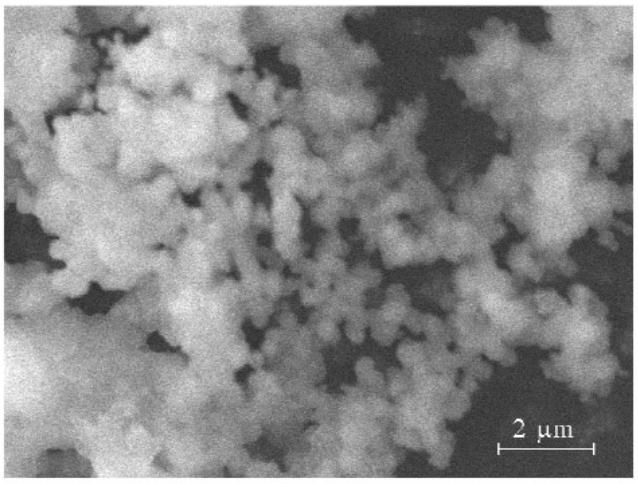

Fig. 4 Synthesized small carbon particles that form large clusters.

In order to quantify the consumption of the precursor gas C_2H_2 for the film deposition onto the MF grains and the C-dust formation, the acetylene molecules were monitored by IR laser diode absorption spectroscopy (TDLAS) [30]. The TDLAS absorption decreases after a very short process duration (about 20 s), which indicates a fast and efficient decomposition of the C_2H_2 molecules (Fig. 5). The dissociated radicals (mainly C_2H) are the precursors for the particle formation, which starts spontaneously in an Ar/C_2H_2 plasma. Similar observations were made by [31]. The small particles are already visible in the laser light after a short time.

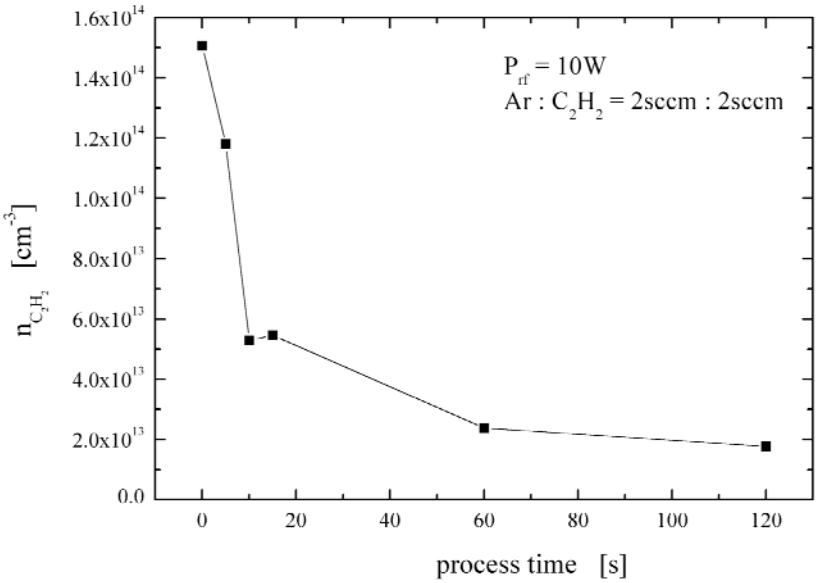

Fig. 5 Decrease of the C_2H_2 concentration owing to the decomposition of the precursor gas as measured by TDLAS.

Simultaneously, the laser light intensity through the plasma remarkably drops owing to the formation of carbon dust in the course of a-C:H deposition (Fig. 6). After about 100 s, an oscillation of the laser light intensity can be observed owing to the dynamics of the carbon dust formation. The growth

mechanism is accompanied by the action of the various forces (particle drop due to gravitation, particle flow due to ion drag, etc.) and the development of voids. This behavior results in alternating dust-free zones and dust zones. After switching off the acetylene supply, the light intensity increases and stabilizes again owing to vanishing particle density, as can be seen in Fig. 6.

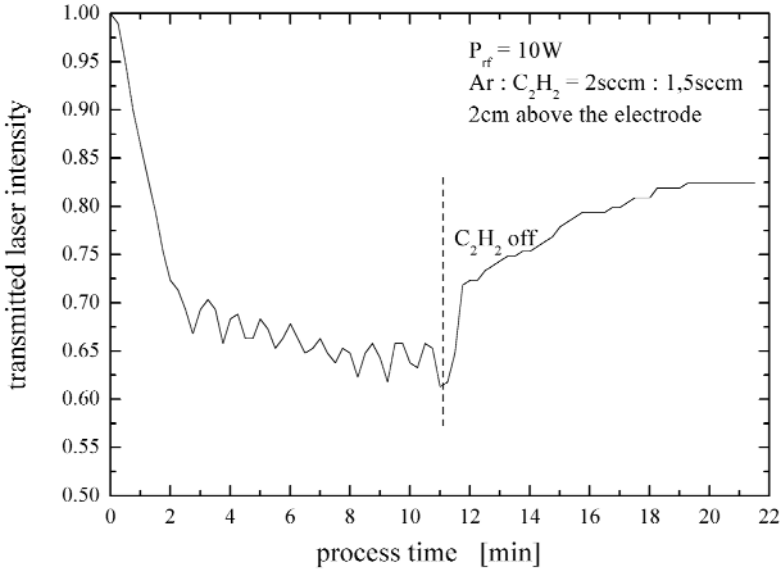

Fig. 6 Decrease and oscillation of the laser light owing to the growth and dynamics of the particles. After stop of C_2H_2 supply, an increasing laser signal can be observed indicating a vanishing particle density.

DEPOSITION OF PROTECTIVE COATINGS ONTO PHOSPHOR PARTICLES

An example for the technological powder treatment in a process plasma is the deposition of alumina coatings on phosphor particles by a plasma-enhanced chemical vapor deposition (PECVD) process. The deposited layers will protect the particles against degradation and aging during plasma and UV irradiation in fluorescent lamps. Thin films of alumina (Al_2O_3) are chemically stable and allow a substantially full light transmission at the excitation wave length of mercury (254 nm) and in the visible range.

For the phosphor particle coating experiment, the metal-organic precursor aluminum-tri-isopropyloxide (ATI) was dissociated in the rf discharge containing an ATI/Ar or ATI/air mixture, respectively. The rf power was varied between 10 and 100 W and the gas flow rate between 0.5 and 10 sccm, corresponding to a pressure of 5–30 Pa. Changes in the electron density during the process were measured by self-excited electron resonance spectroscopy (SEERS, ASI Hercules) [32]. After the decomposition of the ATI [$Al(i\text{-}OC_3H_7)_3$], precursor thin alumina films were deposited surrounding the injected phosphor particles proved by X-ray photoelectron spectroscopy (XPS). The particles are phosphors of high brightness and high maintenance often used as the blue component in a tricolor fluorescent lamp, which consist of $BaMg_2Al_{16}O_{27}:Eu^{2+}$.

Since the ATI fragments tend to form negative ions, the electron density shows only a weak variation with the power, whereas a strong increase in pure argon plasma could be observed (Fig. 7). This observation is due to the electron attachment by the radicals, which contribute to the film growth at the luminophore particles. The electron density in a pure argon plasma rises with increasing power (30–100 W) from $2{\cdot}10^8$ to $12{\cdot}10^8$ cm^{-3}, while the density in an Ar/ATI plasma is about 10^8 cm^{-3}. In the argon plasma, the degree of ionization increases with the discharge power and, hence, the density of Ar^+ ions and electrons rises, too. In ATI or O_2 plasma, respectively, the ionization also increases as a function of the discharge power. However, the electrons are attached to a certain extent at the radicals

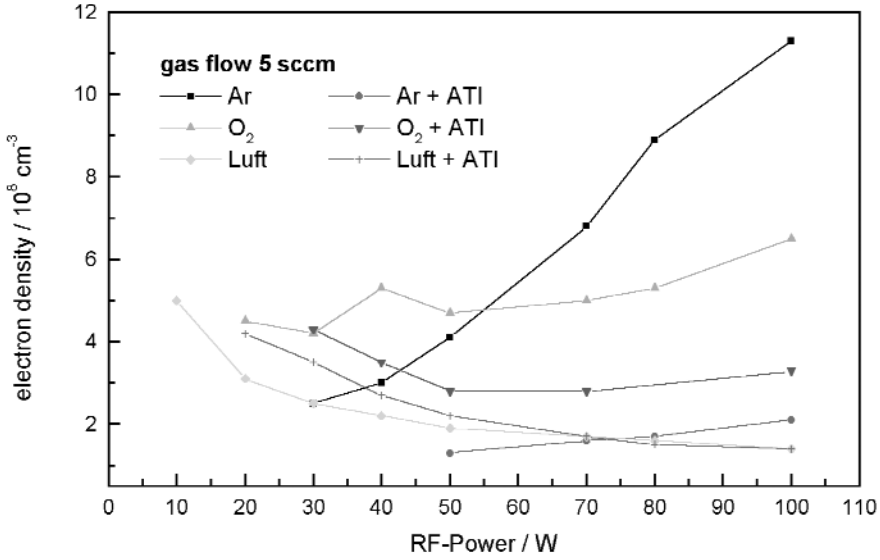

Fig. 7 Electron density as measured by SEERS in dependence on the discharge power.

to form negative ions. As a result, the density of free electrons hardly changes, see Fig. 7. The different order of magnitude and the tendency in the electron densities for the different process conditions allow conclusions with regard to the dissociation and ionization mechanisms and reveal information on thin film deposition on the fluorescent grains.

The original phosphor particles that are not coated by a protective alumina layer show a remarkable decrease in their light intensity after the Ar plasma treatment, which simulates the process conditions in a lamp. Therefore, the particles were coated by the protective alumina layer. The success of the particle deposition was proved by XPS. It could be demonstrated that the luminophore grains show CH groups from the glue before deposition, whereas nearly no CH groups could be detected by XPS at the particles after the deposition of the protective layer. As a result, PECVD by decomposition of ATI in the rf plasma for obtaining transparent Al_2O_3 films onto phosphor particles results in a much higher stability against plasma irradiation, e.g., against UV radiation and particle bombardment at low energies in comparison to the nontreated particles. The light intensity of coated luminophores remains stable even for high plasma power, whereas the light intensity of nontreated luminophores decreases at plasma irradiation at high power, see Fig. 8. This observation is due to the fact that coated particles are more resistent to degradation than noncoated ones.

Since the fluorescent properties of the grains should be preserved, it is important that there is no change by the Al_2O_3 protective layers in the emission spectra of the particles. It could be shown that the emission spectra of the alumina-coated $BaMg_2Al_{16}O_{27}:Eu^{2+}$ do not differ from the uncoated material. An additional advantage of the plasma treatment under optimized conditions (e.g., 30 W, 5 sccm air/ATI, 30 min treatment time) is the decomposition of the glue material, which renders an unnecessary additional annealing process.

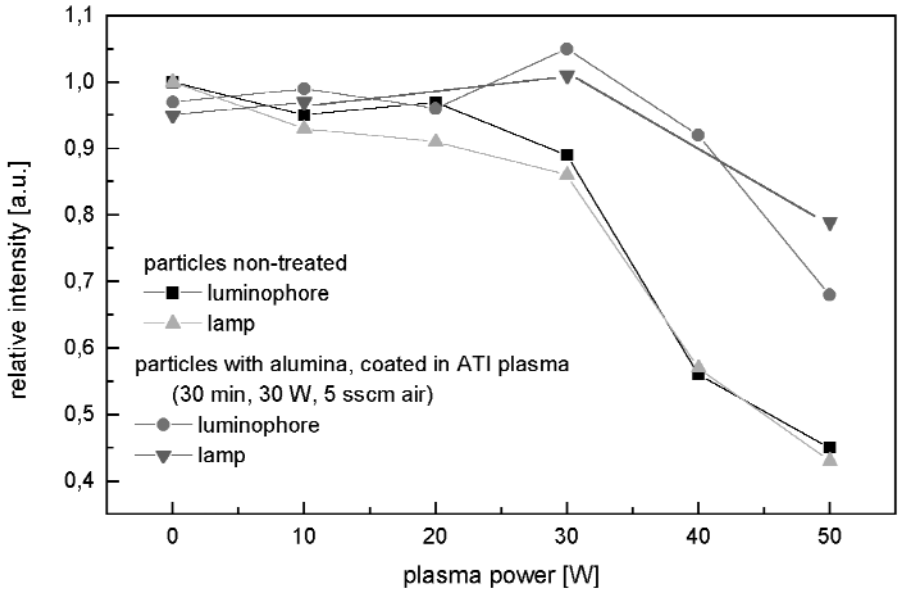

Fig. 8 Comparison of light intensities of noncoated and coated luminophore particles after plasma irradiation.

COATING OF POWDER PARTICLES IN A MAGNETRON DISCHARGE

An approach for the coating of externally injected particles was demonstrated in [9], where an argon rf plasma was employed to charge and confine particles, while a metal coating was performed by means of a separate dc magnetron sputter source. In a quite similar matter, the deposition of different metals onto silica grains is presented, whereas the interaction between the magnetron discharge and the trapped particles was under special investigation.

For the experiments a dc magnetron source (von Ardenne PPS 50) was mounted opposite to the rf electrode (Fig. 2). Typical experimental conditions were: pressure 3–20 Pa, rf power 1–10 W, magnetron power 10–200 W supplied by a generator (Advanced Energy MDX 500). Silicon oxide particles with a diameter of 18 μm were trapped in the sheath above the rf electrode. A copper ring was placed on the rf electrode in order to confine the particles in the center. The planar dc magnetron sputter source was used to deposit thin metallic films on the particles, which served as microsubstrates. Al, Cu, or Ti cathodes, respectively, were used as targets. The distance between the target and the confined particles was about 70 mm. In addition to the diagnostics mentioned above, Langmuir probe measurements were carried out which provided information on the electron component and the plasma potential. The coated particles were examined by SEM. Some pictures of the particles are shown in Fig. 9.

The structure of the metallic films was different, depending on the target material. While the Al and Cu films were deposited rather smoothly, the Ti films showed a distinct island formation. This can be explained by the lower sputter yield of the titanium target and also by the different surface adhesion between the particles and the deposited material [33]. The surface energy of titanium (1.39 J/m^2) is higher than that of aluminum (0.91 J/m^2) and copper and, therefore, the wetting of the particle surface is worse for titanium.

The difference between original and coated powder particles is obvious. The particles are completely covered by close and rather thick metal layers. The modified particles differ from the original ones also in their contrast in the SEM pictures. The metal films were closed on most particles. A good exception is shown in Fig. 9d where the layer is broken probably due to thermal tension. It was possible to estimate the thickness of the deposited copper films to about 1.5 μm from this picture. The coated

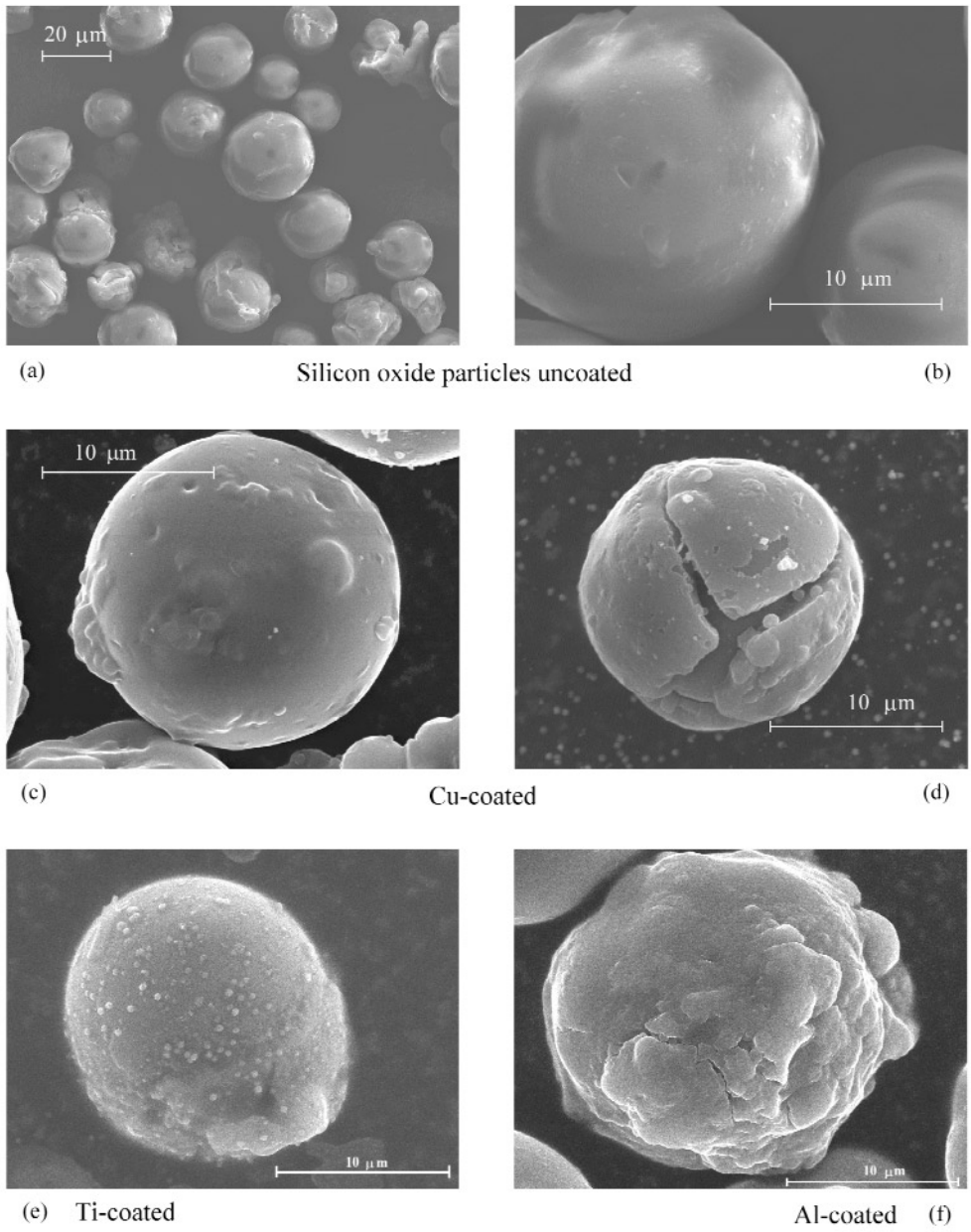

Fig. 9 SEM photographs of silicon oxide particles that were coated by magnetron sputtering.

particles show a rough and cauliflower-like shape, which makes them attractive, especially for catalytic application.

If the deposited films were thinner, the layer surrounding the particles could be smoother as well. In such cases, the surface structure of the coated particles (which was still completely closed) looked more golfball-like, which might be interesting for optical application [9].

It is only possible to trap about 10^5 particles per cubic centimeter in the used experimental set-up. This corresponds to a mass of about 0.5 mg. The particles were treated in the magnetron discharge for about 5 min. The metallic layers were deposited quite evenly on all particles. That renders a yield of coated particles of about 50 mg/h if it were possible to extract the particles directly from the reactor

through some kind of load-lock system. It is rather little, but can probably be enhanced by a scaled set-up.

An interesting observation was made during the magnetron experiments: when the magnetron was turned on, the entire particle cloud began to rotate, see Fig. 10. After the magnetron was turned off, the rotation ceased fast owing to the neutral drag. Similar observations of particle motion under the influence of a permanent magnetic field were made by Konopka et al. [34]. They explain the rotation with the azimuthal component of the ion drag force due to ***ExB***-drift of the ions in the perpendicular radial electric and vertical magnetic field.

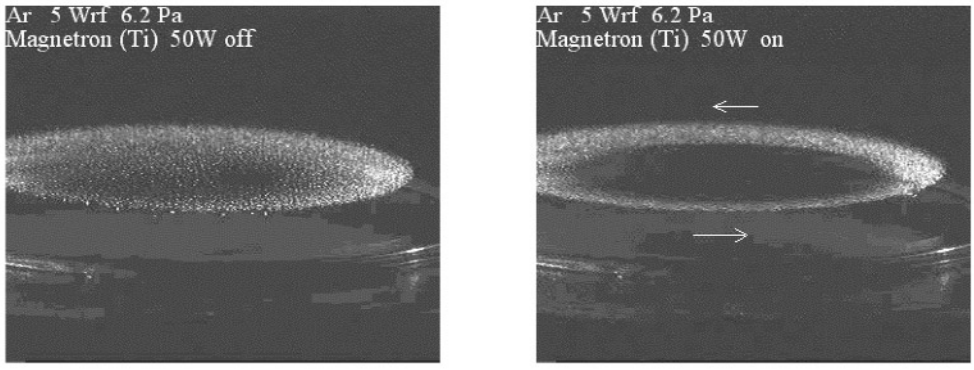

Fig. 10 Particle cloud before and after the magnetron was turned on.

However, the particle cloud rotation was observed only under the influence of the magnetron discharge. That means for this effect the interaction of the rf plasma and the magnetron discharge is significant. The magnetic field of the permanent magnets in the magnetron is very weak in the particle distance ($B_{z,Mag} \approx 10^{-4}$ T) and had no impact on the particles solely.

The rotation of the particle cloud is ascribed to momentum transfer through collisions of the plasma ions with the particles [22]. The ions are accelerated through ***ExB*** drift in the perpendicular vertical component of the permanent magnetic field $B_{z,Mag}$ of the magnetron and the radial component of the electric field above the rf electrode. The latter is caused by a flow of electrons from the magnetron plasma, which changes the potential distribution in the region where the particles are trapped. In front of the magnetron target there exists a ring-shaped region of high electron density owing to the magnetic field. Electrons constantly drift down from there. This explanation is illustrated in Fig. 11. Langmuir probe measurements confirm these assumptions. They show an increase of the electron density as well as a maximum of the plasma potential in the center of the electrode. The resulting electrical fields are in the order of 50 V/m.

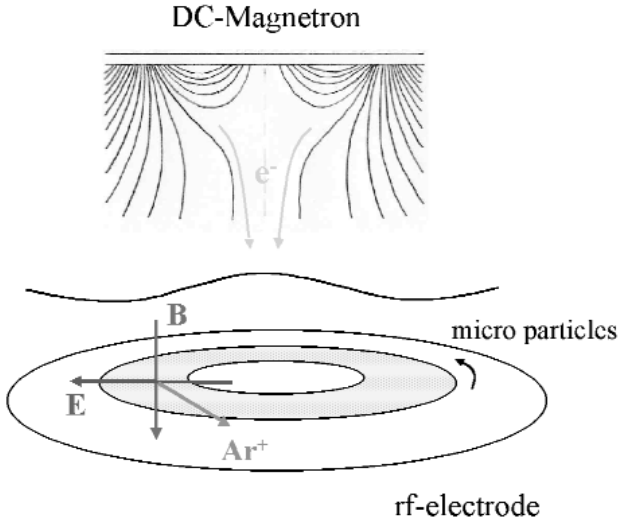

Fig. 11 Illustration of the fields causing by tangential ion drag the rotation of the particle cloud at magnetron operation.

The motion of the particle cloud was studied in dependence on various parameters. The rotation frequency increases linearly with rising magnetron power, accounting for the increase of the charge carrier density in the magnetron discharge. This observation supports our supposition of the influence of the electron ring current, since the density of the charge carriers increases with the magnetron discharge power. Also, the dependence on the gas pressure was studied (Fig. 12). The rotation frequency f_{rot} decreases with increasing pressure p, which can be explained with the rising neutral friction force F_N (neutral drag).

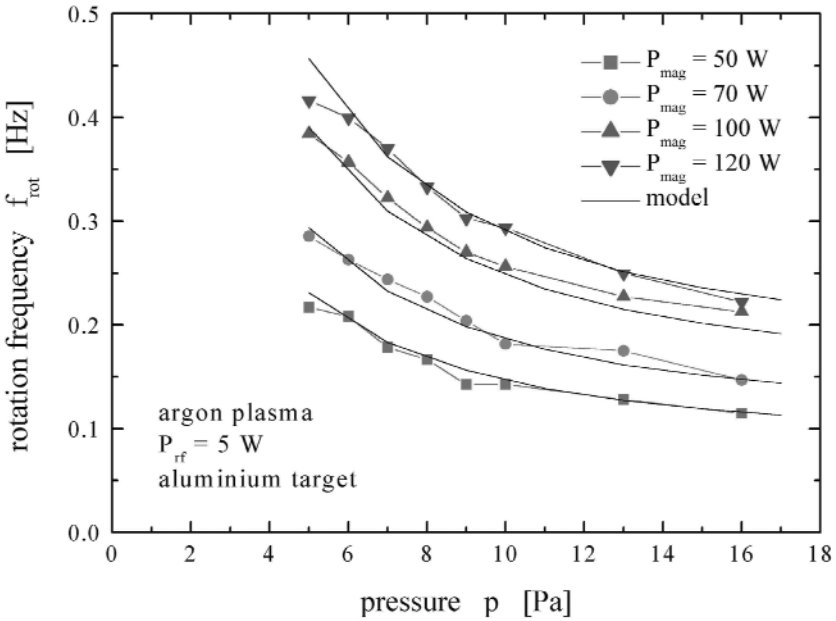

Fig. 12 Pressure dependence of the rotation frequency of the particle cloud at different power.

For the rotation frequency, the force balance between the ion drag F_{ion} and the neutral drag F_N [35] is important:

$$F_N = \xi p v_S = F_{ion}$$

where p is the gas pressure, $v_S = 2\pi r_S f_{rot}$ is the rotation velocity of the particle cloud, r_S is the mean radius of the rotating particle cloud, and ξ is a parameter depending on the gas and the particles.

By that, the following expression for the rotation frequency can be derived [36,37]:

$$f_{rot} = \frac{\left(\sigma_{coll} + \sigma_{coul}\right) n_i \left(p, P_{mag}\right) m_{Ar} v_{di} \sqrt{v_{di}^2 + v_{th,i}^2}}{2\ r_S \zeta} \cdot \frac{1}{p}$$

where σ_{coll} is the collision cross-section for ion momentum transfer, σ_{coul} is the cross-section for Coulomb interaction, n_i is the ion density, m_{Ar} is the ion mass, v_{di} is the drift velocity of the ions, and $v_{th,i}$ is the thermal velocity of the ions.

Figure 12 shows the comparison of the experimental data points and the model, which agree quite well.

CONCLUSION

Powder synthesis, trapping, modification, and coating in laboratory discharges have gained growing interest in the past decade. There are possibilities for the coating of powder particles for technological applications as it was demonstrated.

Nanosized carbon particles were produced in the course of amorphous film deposition. The synthesized particles show a uniform size distribution, which makes them attractive for incorporation into thin films.

Luminophore grains were coated by a protective alumina layer in a metal-organic PECVD process. The treated particles show a better stability in their light intensity, i.e., the surface properties with regard to the degradation by plasma irradiation could be remarkably improved. Furthermore, small SiO_2 grains were coated by thin metallic films in a combined plasma configuration of an rf plasma for particle charging and trapping, and a dc magnetron sputter source for deposition. However, the amount of the confined particles and, thus, the yield of modified powder are still rather small and have to be increased for a reasonable industrial application.

The interaction between process plasma and injected microdisperse powder particles can be used also as a diagnostic tool for the study of plasma surface mechanisms in low-pressure plasmas. For example, in magnetron sputtering of thin films onto dust grains, the observation and interpretation of the rotation of the particle cloud under the influence of the magnetron discharge reveals information on the electron flux pattern as well as on the neutral and ion drag.

The presented examples emphasize that the technological application of complex plasmas is a promising field of research in the frontier area between plasma physics, material processing, and diagnostics.

ACKNOWLEDGMENT

This work was partly supported by the Deutsche Forschungsgemeinschaft (DFG) under SFB198/A14. The authors gratefully acknowledge M. Hähnel, A. Knuth, and Mrs. C. Krcka for their support.

REFERENCES

1. G. S. Selwyn, J. S. McKillop, K. L. Haller, J. J. Wu. *J. Vac. Sci. Technol.* **A8**, 1726 (1990).
2. A. Bouchoule (Ed.). *Dusty Plasmas: Physics, Chemistry and Technological Impacts in Plasma Processing*, John Wiley, New York (1999).
3. E. Stoffels, W. W. Stoffels, H. Kersten, G. H. P. M. Swinkels, G. M. W. Kroesen. *Phys. Scripta* **T89**, 168 (2001).
4. D. A. Law, E. B. Tomme, W. H. Steel, B. M. Anaratonne, J. E. Allen. In *Proceedings of the XXIV ICPIG*, proc. IV/109 Warsaw, Poland, 1999.
5. G. H. P. M. Swinkels, H. Kersten, H. Deutsch, G. M. W. Kroesen. *J. Appl. Phys.* **88**, 1747 (2000).
6. H. Kersten, H. Deutsch, E. Stoffels, W. W. Stoffels, G. M. W. Kroesen. *Int. J. Mass Spectrom.* **223–224**, 313 (2003).
7. G. S. Selwyn, J. Singh, R. S. Benett. *J. Vac. Sci. Technol*. **A7**, 2758 (1988).
8. A. Bouchoule. *Phys. World* **6**, 47 (1993).
9. H. Kersten, P. Schmetz, G. M. W. Kroesen. *Surf. Coat. Technol*. **108/109**, 507 (1998).
10. U. Kogelschatz, B. Eliasson, W. Egli. *Pure Appl. Chem*. **71**, 1819 (1999).
11. N. Rao, S. Girshick, J. Heberlein, P. McMurray, S. Jones, D. Hansen, B. Micheel. *Plasma Chem. Plasma Proc*. **15**, 581 (1995).
12. H. S. Shin and D. G. Goodwin. *Mater. Lett*. **19**, 119 (1994).
13. M. Karches, C. Bayer, P. R. von Rohr. *Surf. Coat. Technol*. **119**, 879 (1999).
14. A. A. Howling, L. Sansonnens, J. L. Dorier, C. Hollenstein. *J. Appl. Phys*. **75**, 1340 (1994).
15. T. Ishigaki, T. Sato, Y. Moriyoshi, M. I. Boulos. *J. Mater. Sci. Lett.* **14**, 1694 (1995).
16. K. Kitamura, S. Akutsu, S. Ito, K. Akashi. In *Proceedings of the ICRP-3*, proc. 357, Nara, Japan, 1997.
17. P. Roca I Cabarocas, P. Gay, A. Hadjadj. *J. Vac. Sci. Technol.* **A14**, 655 (1996).
18. S. Veprek. *Pure Appl. Chem*. **68**, 1023 (1996).
19. B. Schultrich, H. J. Scheibe, H. Mai. *Adv. Eng. Mater*. **2**, 419 (2000).
20. E. Stoffels, W. W. Stoffels, G. Ceccone, F. Rossi. *J. Vac. Sci. Technol.* **A17**, 3385 (1999).
21. S. Yan, H. Maeda, J. I. Kusakabe, K. Morooka, T. Okubo. *J. Mater. Sci.* **28**, 1829 (1993).
22. H. Kersten, R. Wiese, G. Thieme, M. Fröhlich, A. Kopitov, D. Bojic, F. Scholze, H. Neumann, M. Quaas, H. Wulff, R. Hippler. *New J. Phys*. 5 (2000).
23. E. B. Tomme, D. A. Law, B. M. Annaratone, J. E. Allen. *Phys. Rev. Lett.* **85**, 2518 (2000).
24. J. E. Daugherty and D. B. Graves. *J. Vac. Sci. Technol*. **A11**, 1126 (1993).
25. H. Kersten, H. Deutsch, M. Otte, G. H. P. M. Swinkels, G. M. W. Kroesen. *Thin Solid Films* **377–378**, 530 (2000).
26. H. Thomas, G. E. Morfill, V. Demmel, J. Goree, B. Feuerbacher, D. Möhlmann. *Phys. Rev. Lett.* **73**, 652 (1994).
27. A. Melzer, A. Homann, A. Piel. *Phys. Rev*. **E53**, 2757 (1996).
28. K. Tachibana and Y. Hayashi. *Pure Appl. Chem*. **68**, 1107 (1996).
29. F. Vivet, A. Bouchoule, L. Boufendi. In *Proceedings of the ICRP-XXXIII*, proc. I/200, Toulouse, France, 1997.
30. J. Röpcke, L. Mechold, M. Käning, J. Anders, F. G. Wienhold, M. Zahniser. *Rev. Sci. Instrum*. **71**, 3706 (2000).
31. S. Hong, J. Berndt, J. Winter. In *Proceedings of the ICPDP-2002*, p. 305, Durban, South Africa, 2002.
32. M. Klick. *J. Appl. Phys*. **79**, 3445 (1996).
33. F. Vollertsen and S. Vogler. *Werkstoffeigenschaften und Mikrostruktur*, Hanser-Verlag, München (1989).
34. U. Konopka, D. Samsonov, A. V. Ivlev, J. Goree, V. Steinberg. *Phys. Rev*. **E61**, 1890 (2000).
35. P. S. Epstein. *Phys. Rev*. **23**, 710 (1924).

36. M. S. Barnes, J. H. Keller, J. C. Foster, J. A. O'Neill, D. K. Coultas. *Phys. Rev. Lett.* **68**, 313 (1992).
37. M. D. Kilgore, J. E. Daugherty, R. K. Porteous, D. B. Graves. *J. Appl. Phys.* **73**, 7195 (1993).